

$W\gamma$ production in vector boson fusion at NLO in QCD

Francisco Campanario,^{1,*} Nicolas Kaiser,^{2,†} and Dieter Zeppenfeld^{2,‡}¹*Theory Division, IFIC, University of Valencia-CSIC, E-46980 Paterna, Valencia, Spain.*²*Institute for Theoretical Physics, KIT, 76128 Karlsruhe, Germany.*

The next-to-leading order QCD corrections to $W^\pm\gamma$ production in association with two jets via vector boson fusion are calculated, including the leptonic decay of the W with full off-shell effects and spin correlations. The process lends itself to a test of quartic gauge couplings. The next-to-leading order corrections reduce the scale uncertainty significantly and show a non-trivial phase space dependence.

PACS numbers: 12.38.Bx, 13.85.-t, 14.70.Fm, 14.70.Bh

Di-boson production processes in association with two jets play an important role at the LHC, not only as a background to searches for physics beyond the Standard Model, but also as a means to test the structure of the electroweak symmetry breaking sector. Within the Standard Model (SM), there are three distinct production modes at leading order (LO). The QCD mechanism, i.e. the radiation of two partons in quark-antiquark annihilation to two vector bosons and crossing related processes, is of order $\mathcal{O}(\alpha_s^2\alpha^2)$ for on-shell production of both gauge bosons. For these processes, results at NLO QCD have been reported for W^+W^-jj [1, 2], $W^+W^\pm jj$ [3], $W^\pm Zjj$ [4], including the leptonic decay of the vector bosons with all off-shell effects, and $\gamma\gamma jj$ [5] production. In addition, there is the “vector-boson-fusion” (VBF) mechanism, which is of order $\mathcal{O}(\alpha^4)$ at LO for on-shell production. The basic subprocess for the VBF channel is vector boson scattering, which means that the VBF processes are particularly interesting as a probe of electroweak symmetry breaking. For weak boson scattering, the main focus will be on the scattering of longitudinal W’s and Z’s and the question, whether the recently discovered Higgs boson does indeed unitarize this process. However, electroweak boson scattering is also an excellent source of information on trilinear and quartic gauge couplings, and here, probing the scattering of transversely polarized gauge bosons is as important as the scattering of longitudinal modes. When considering transverse polarizations, final state photons are just as interesting as Z-bosons or W’s. Finally, the production of three electroweak gauge bosons, with one off-shell gauge boson decaying into a quark-antiquark pair, is a third source of $VVjj$ events at order $\mathcal{O}(\alpha^4)$. NLO QCD corrections to VVV production with leptonic decays are available via the VBFNLO program [6]. Since the above three production modes peak in different regions of phase space, and because of their largely orthogonal color structures, interference between these modes is generally unimportant and can be neglected in most applications.

NLO QCD corrections for the VBF processes have been provided for all combinations of massive di-boson production in Refs. [7–11]. In this letter, we present

the first theoretical prediction for the VBF production of $W^\pm\gamma jj$ final states at order $\mathcal{O}(\alpha_s\alpha^5)$. Compared to a massive gauge boson, which typically is observed in leptonic decays with a small branching fraction of order 3 to 10 %, the production cross section of a final state on-shell photon is considerably enhanced. In our calculation, the leptonic decay of the W boson is consistently included, with all off-shell effects and spin correlations taken into account. This includes also final state radiation, i.e. the radiative decay of the W. Radiative W decays provide a sizable source of $\ell\nu\gamma jj$ events which diminish the sensitivity of $W\gamma jj$ production to anomalous couplings. In this letter, we also study how these contributions can be reduced safely. In the following, we consider the specific leptonic final state $e^\pm(\bar{\nu}_e)\gamma$. The final results can be multiplied by a factor two to take the $\mu^\pm(\bar{\nu}_\mu)\gamma$ channel into account.

This letter is organized as follows: After this introduction, we will explain the major points of the implementation of $W^\pm\gamma jj$ production into the Monte-Carlo program VBFNLO [6] and the checks that we performed to assure its correctness. Then, the setup used for the calculation and the numerical results for the cross sections will be given. We will show that calculating the NLO QCD corrections reduces the scale uncertainty and that these corrections have a non-trivial phase space dependence. Finally, we will demonstrate how to suppress the contributions from radiative W decay.

CALCULATIONAL METHOD

Our calculation of the $W^\pm\gamma jj$ production cross section at NLO QCD closely follows the one for $W^\pm Zjj$ production [9] and other VBF channels implemented in VBFNLO [6]. We consider only t-channel and u-channel Feynman diagrams but neglect interference between them. s-channel contributions, i.e. $VW\gamma$ production with subsequent hadronic decay of the (off-shell) V are considered a separate process in VBFNLO. Contributions from s-channel diagrams as well as interference terms between t-, u-, and s-channel contributions are

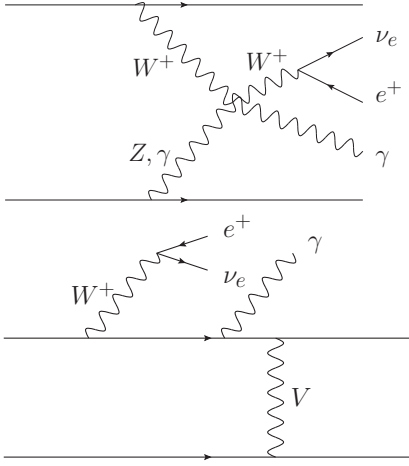


FIG. 1: Representative tree-level Feynman diagrams.

strongly suppressed by the VBF cuts that we apply in this letter. For the calculation of the LO Feynman diagrams, e.g. the ones shown in Fig. 1, the spinor-helicity formalism of Ref. [12] is used. The electroweak parts of the diagram are combined to so-called leptonic tensors, which have to be calculated only once per phase space point. For the calculation of the leptonic tensors, we use the routines of the *HELAS* package [13]. The real emission (RE) contributions comprise $q \rightarrow qg$ sub-diagrams, for example the ones that arise if one adds one gluon at every possible spot to the diagrams in Fig. 1, as well as the corresponding $g \rightarrow q\bar{q}$ diagrams. For the construction of the RE diagrams, we use the same strategy as for the LO ones. For the virtual amplitudes, we

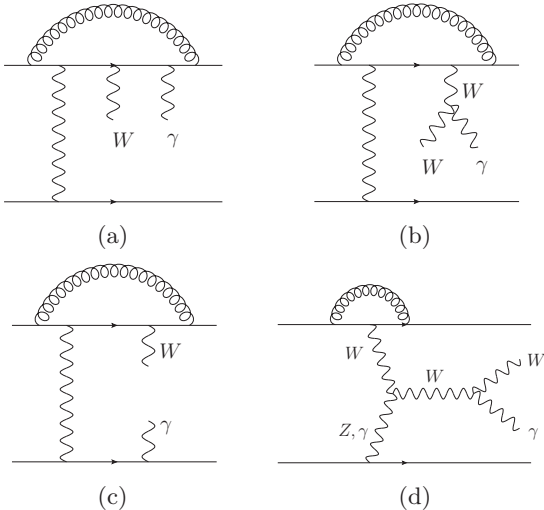


FIG. 2: Selected Feynman diagrams contributing to the virtual amplitudes.

do not consider gluon exchange between the two quark lines. For the square of t-, u- or s-channel diagrams such

contributions vanish due to color conservation. For interference terms, their contributions are also suppressed by the VBF cuts. Then, the virtual correction diagrams are obtained by adding a gluon loop over each possible combination of the internal propagators and the external legs of a single quark line of the LO diagrams. The lower diagram in Fig. 1 gets virtual corrections up to a pentagon on the upper line as depicted in Fig. 2a. Its lower line obtains only vertex corrections similarly to the VBF Feynman diagram in Fig. 2d. In addition, there are several box diagrams, e.g. the ones presented in Fig. 2b and Fig. 2c. The box correction in the latter one can also be on the lower line. All the virtual corrections to one quark line up to boxes or pentagons were calculated using the *Boxline* or *Penline* routines of Ref. [14], respectively. For the regularization of the infrared divergences, we use dimensional reduction and the Catani-Seymour dipole subtraction method [15] to make the virtual and the real emission contributions numerically integrable in four dimensions. The subtraction procedure follows the one in Ref. [16] and, hence, allows us to use an individual scale for each quark line. We calculate the Born matrix elements, which are needed for the calculation of the subtraction terms for $q \rightarrow qg$ and $\bar{q} \rightarrow \bar{q}g$ splitting, and cache them, so we can reuse them in the $g \rightarrow q\bar{q}$ case. Furthermore, we include anomalous couplings effects, which will be studied in a forthcoming paper.

For the potentially resonating W^\pm and Z propagators we use a variant of the complex mass scheme as implemented in MADGRAPH [17]. We checked our tree level matrix elements against MADGRAPH and compared the cross sections to SHERPA [18]. Applying VBF cuts, we found complete agreement for the two jet cross sections but deviations of 1.5% and 4% for $W^+\gamma jjj$ and $W^-\gamma jjj$ production respectively. We checked explicitly that these deviations originate from the neglected s-channel contributions. They contribute at the per mille level to the total NLO QCD corrections to $W^\pm\gamma jjj$ production and, therefore, can be safely neglected. The final state photon offers us the possibility to perform gauge tests which are satisfied by all contributions.

Furthermore, the known [14] analytic expression of the poles for multiple vector boson emissions (on-shell or off-shell) along a quark line has been compared numerically with the coefficients of the $1/\epsilon$ and $1/\epsilon^2$ poles computed in our process with the *Boxline* and *Penline* routines. One typically finds agreement to 10 to 14 digits, thus, providing an additional strong check of the correctness of the implementation. In order to assure the numerical stability of the calculation of the virtual contributions, we use Ward identity checks. We set the amplitude to zero if the Ward identities are satisfied with a precision worse than $\epsilon = 0.01$. The share of phase space points, in which the Ward tests fail, is 0.36% for the *Penlines* and $1.6 \cdot 10^{-6}\%$ for the *Boxlines*. Since the total NLO contributions are at the level of a few per cent, the er-

ror induced by setting the virtual amplitude to zero for those points is well below the statistical error, and, thus, negligible.

We checked the convergence of the dipoles of the Catani-Seymour subtraction. Moreover, we shifted parts of the terms proportional to $|\mathcal{M}_B|^2$ from the five particle phase space of the virtual corrections to the six particle phase space of the real emission and found agreement within the numerical accuracy.

NUMERICAL RESULTS

As EW input parameters, we use $M_Z = 91.1876$ GeV, $M_W = 80.398$ GeV and $G_F = 1.16637 \times 10^{-5}$ GeV $^{-2}$ and derive the weak-mixing angle using the SM tree-level relations. All fermions aside from the top quark are considered to be massless. The width of the Z and the W bosons are calculated to be $\Gamma_Z = 2.508$ GeV and $\Gamma_W = 2.098$ GeV respectively. We use the CTEQ6L1 and CT10 parton distribution functions (PDF) [19] at LO and NLO respectively with $\alpha_s^{\text{LO}}(M_Z) = 0.129808$ and $\alpha_s^{\text{NLO}}(M_Z) = 0.117982$. The numerical results presented in this letter are calculated in the four-flavor scheme for the LHC at 14 TeV center-of-mass energy. Effects from generation mixing are neglected [9] since they almost completely cancel due to the unitarity of the CKM-matrix. To reduce the contamination of s-channel contributions, we apply typical VBF cuts. The charged lepton and photon are required to be hard and central: $p_{T,\ell(\gamma)} \geq 20(30)$ GeV and $|y_{\ell(\gamma)}| \leq 2.5$. Final state partons are clustered to jets using the anti- k_t algorithm [20] with the radius $R = 0.4$. There must be at least two hard jets with $p_{T,\text{jet}} \geq 30$ GeV and $|y_{\text{jet}}| \leq 4.5$. In addition, we impose a requirement on the lepton-jet and photon-jet separation in the azimuthal angle-rapidity plane $\Delta R_{\ell,j} \geq 0.4$ and $\Delta R_{\gamma,j} \geq 0.7$, where only jets passing the above cuts are considered. Furthermore, we use the photon isolation criterion à la Frixiene [21] with a cone radius of $\delta_0 = 0.7$, efficiency $\epsilon = 1$ and exponent $n = 1$. The VBF cuts, which we apply, are $|y_{j1} - y_{j2}| > 4$, $y_{j1} \times y_{j2} < 0$ and $m_{j1 j2} > 600$ GeV. As the central value for the factorization and renormalization scales, we choose $\mu_{Fi} = \mu_{Ri} = \mu_0 = Q_i$, where Q_i is the absolute value of the momentum transferred from quark line i to the EW process. With this setup, we obtain $\sigma_{LO} = 7.828 \pm 0.005$ fb (4.486 ± 0.003 fb) and $\sigma_{NLO} = 7.910 \pm 0.007$ fb (4.588 ± 0.005 fb) for $W^+\gamma jj$ ($W^-\gamma jj$) production, with the W decaying into the first generation of leptons. The K-factor, defined as $K \equiv \sigma_{NLO}/\sigma_{LO}$, is 1.013 (1.021). Since we calculate only a fixed order in perturbative QCD, our results depend on two unphysical scales, the factorization scale μ_{Fi} and the renormalization scale μ_{Ri} . The scale variation plot in Fig. 3 shows that the scale dependence of both processes can be significantly reduced

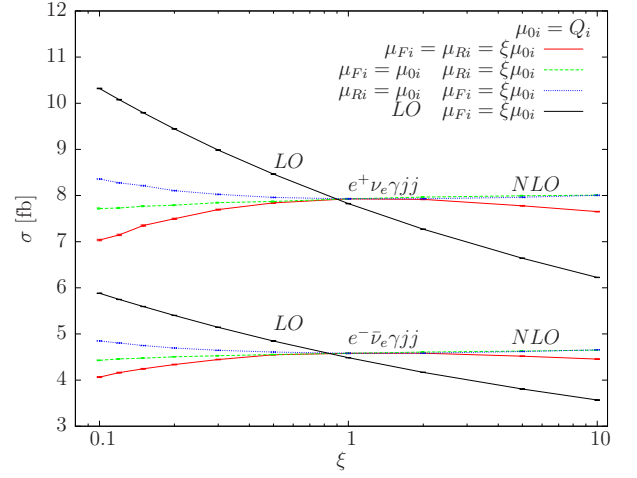


FIG. 3: Scale dependence of the LO and NLO cross sections at the LHC. The lower and upper curves stand for $pp \rightarrow e^- \bar{\nu}_e \gamma jj + X$ and $pp \rightarrow e^+ \nu_e \gamma jj + X$ production, respectively, at a c.m. energy of 14 TeV.

by calculating the NLO QCD corrections.

In the following, distributions for the $W^+\gamma jj$ production channel will be presented. Fig. 4 shows the differential LO and NLO cross sections over the transverse momentum of the hardest jet (upper plot) and the photon (lower plot) as well as the differential and the total K factors. To give a measure for the scale uncertainty, we also plot the results for $\mu_{Fi} = \mu_{Ri} = \mu_{0i} = 2^{\pm 1} Q_i$ (dashed lines). In the $p_{T,j1}$ and the $p_{T,\gamma}$ distributions, the relative scale uncertainty is approximately constant over the whole range examined. In both cases, it can be significantly reduced by calculating the NLO QCD results. While the differential K-factor in the $p_{T,\gamma}$ distribution is stable over the whole range examined, in the $p_{T,j1}$ distribution it decreases continuously over the whole range.

In processes with at least one lepton and one photon in the final state, the photon can be radiated off the lepton. This radiative W decay represents a simple QED process, which diminishes the sensitivity to anomalous couplings in our case. In order to suppress radiative W decay, we follow Ref. [22] and define the transverse cluster mass of the $W\gamma$ system as $m_{T,W\gamma} = \left(\left[(m_{l\gamma}^2 + p_{T,l\gamma}^2)^{\frac{1}{2}} + \not{p}_T \right]^2 - (\mathbf{p}_{T,l\gamma} + \mathbf{p}_T)^2 \right)^{\frac{1}{2}}$. The upper panel in Fig. 5 shows the corresponding distribution. By imposing the cut $m_{T,W\gamma} > 90$ GeV, the radiative decay peak at $m_{T,W\gamma} = m_W$ can be removed. This cut reduces the final state radiation contributions significantly and affects mainly the region of small $R_{l\gamma}$ (lower panel). Additionally, the NLO cross section is only reduced by approximately 10%, which shows the efficiency of the cut.

In this letter, we have presented the first calculation of $W^\pm \gamma jj + X$ production in VBF at order $\mathcal{O}(\alpha_s \alpha^5)$. The

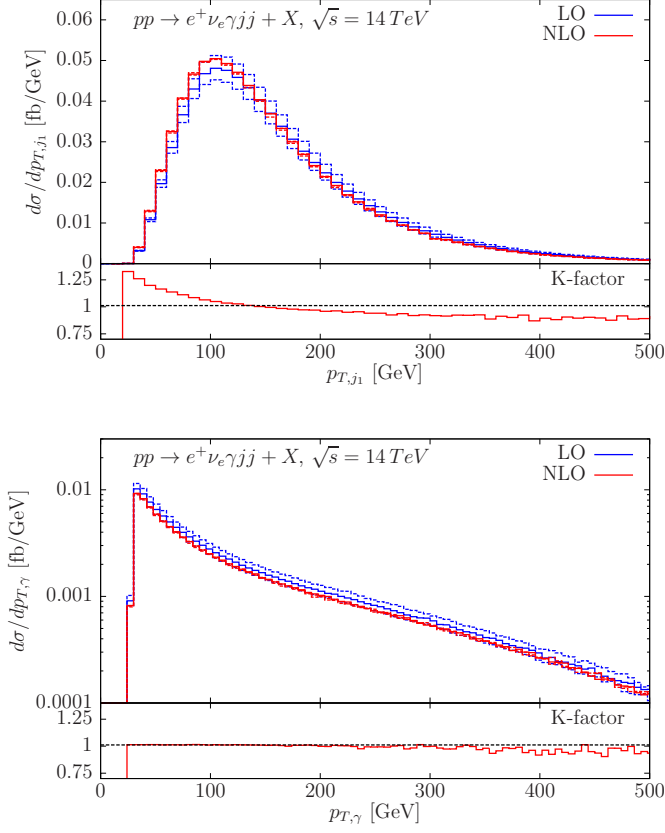


FIG. 4: Differential cross sections and K-factors for the transverse momentum of the hardest jet (top) and the photon (bottom). The dashed lines indicate the results for $\mu_{Fi} = \mu_{Ri} = \mu_{0i} = 2^{\pm 1} Q_i$.

factorization and scale uncertainties at NLO are significantly reduced and one finds K-factors close to one. We plan to make the code publicly available as part of the VBFNLO program [6].

We acknowledge the support from the Deutsche Forschungsgemeinschaft via the Sonderforschungsbereich/Transregio SFB/TR-9 Computational Particle Physics. FC is funded by a Marie Curie fellowship (PIEF-GA-2011-298960) and partially by MINECO (FPA2011-23596) and by LHCPHENONET (PITN-GA-2010-264564).

* francisco.campanario@ific.uv.es

† nicolas.kaiser@student.kit.edu

‡ dieter.zeppenfeld@kit.edu

- [1] T. Melia, K. Melnikov, R. Rontsch, and G. Zanderighi, Phys.Rev. **D83**, 114043 (2011).
- [2] N. Greiner *et al.*, Phys.Lett. **B713**, 277 (2012).
- [3] T. Melia, K. Melnikov, R. Rontsch, and G. Zanderighi, JHEP **1012**, 053 (2010).

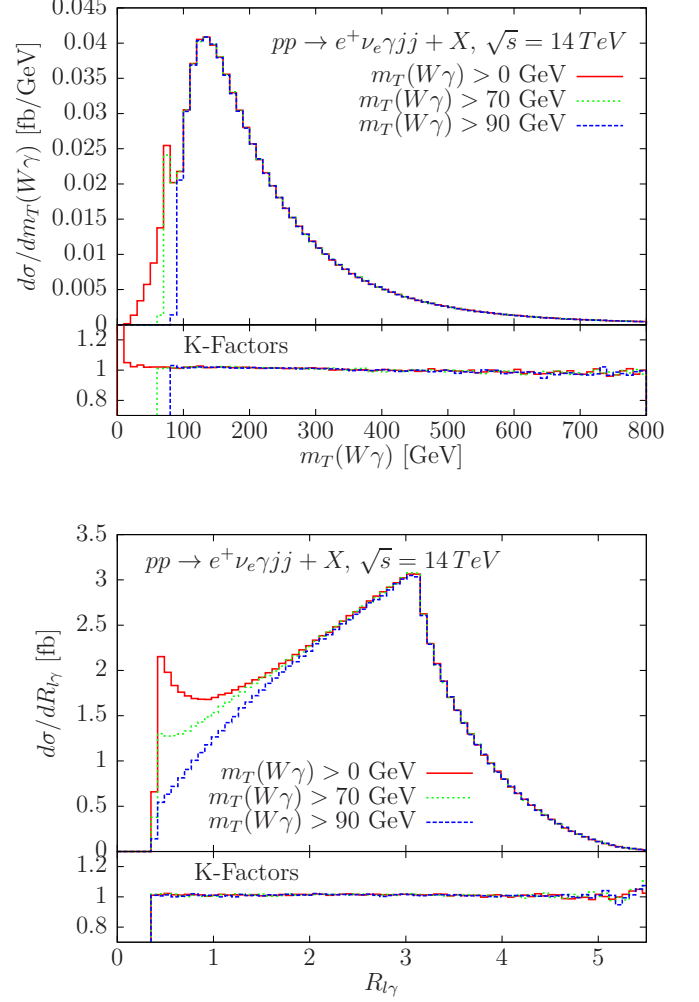


FIG. 5: Differential distribution of the transverse mass of the two gauge bosons $m_{T,W\gamma}$ (upper plot) and differential lepton-photon R separation distribution (lower plot) for different values of the $m_{T,W\gamma}$ cut. Lower panels show the corresponding differential K-factors.

- [4] F. Campanario, M. Kerner, L. D. Ninh, and D. Zeppenfeld, (2013), 1305.1623.
- [5] T. Gehrmann, N. Greiner, and G. Heinrich, (2013), 1308.3660.
- [6] K. Arnold *et al.*, Comput.Phys.Commun. **180**, 1661 (2009).
- [7] K. Arnold *et al.*, (2012), arXiv:1207.4975.
- [8] B. Jager, C. Oleari, and D. Zeppenfeld, JHEP **0607**, 015 (2006).
- [9] B. Jager, C. Oleari, and D. Zeppenfeld, Phys.Rev. **D73**, 113006 (2006).
- [10] G. Bozzi, B. Jager, C. Oleari, and D. Zeppenfeld, Phys.Rev. **D75**, 073004 (2007).
- [11] B. Jager, C. Oleari, and D. Zeppenfeld, Phys.Rev. **D80**, 034022 (2009).
- [12] A. Denner, L. Hosekova, and S. Kallweit, Phys.Rev.

- D86**, 114014 (2012).
- [12] K. Hagiwara and D. Zeppenfeld, Nucl.Phys. **B313**, 560 (1989).
 - [13] H. Murayama, I. Watanabe, and K. Hagiwara, (1992).
 - [14] F. Campanario, JHEP **1110**, 070 (2011).
 - [15] S. Catani and M. Seymour, Phys.Lett. **B378**, 287 (1996), hep-ph/9602277.
 - [16] T. Figy, C. Oleari, and D. Zeppenfeld, Phys.Rev. **D68**, 073005 (2003), hep-ph/0306109.
 - [17] J. Alwall *et al.*, JHEP **0709**, 028 (2007).
 - [18] T. Gleisberg *et al.*, JHEP **0902**, 007 (2009), 0811.4622.
 - [19] A. Martin, W. Stirling, R. Thorne, and G. Watt, Eur.Phys.J. **C63**, 189 (2009).
 - [20] M. Cacciari, G. P. Salam, and G. Soyez, JHEP **0804**, 063 (2008).
 - [21] S. Frixione, Phys.Lett. **B429**, 369 (1998), hep-ph/9801442.
 - [22] U. Baur, T. Han, and J. Ohnemus, Phys.Rev. **D48**, 5140 (1993), hep-ph/9305314.